

# Three-dimensional Resonance in superconducting BaFe<sub>1.9</sub>Ni<sub>0.1</sub>As<sub>2</sub>

Songxue Chi,<sup>1</sup> Astrid Schneidewind,<sup>2</sup> Jun Zhao,<sup>1</sup> Leland W. Harriger,<sup>1</sup> Linjun Li,<sup>3</sup> Yongkang Luo,<sup>3</sup> Guanghan Cao,<sup>3</sup> Zhu'an Xu,<sup>3</sup> Micheal Loewenhaupt,<sup>2</sup> Jiangping Hu,<sup>4</sup> and Pengcheng Dai<sup>1,5,\*</sup>

<sup>1</sup> *Department of Physics and Astronomy, The University of Tennessee, Knoxville, Tennessee 37996-1200, USA*

<sup>2</sup> *Technische Universität Dresden, Institut für Festkörperphysik, 01062 Dresden, Germany*

<sup>3</sup> *Department of Physics, Zhejiang University, Hangzhou 310027, China*

<sup>4</sup> *Department of Physics, Purdue University, West Lafayette, Indiana 47907, USA*

<sup>5</sup> *Neutron Scattering Science Division, Oak Ridge National Laboratory, Oak Ridge, Tennessee 37831-6393, USA*

We use inelastic neutron scattering to study magnetic excitations of the FeAs-based superconductor BaFe<sub>1.9</sub>Ni<sub>0.1</sub>As<sub>2</sub> above and below its superconducting transition temperature  $T_c = 20$  K. In addition to gradually open a spin gap at the in-plane antiferromagnetic ordering wavevector  $(1, 0, 0)$ , the effect of superconductivity is to form a three dimensional resonance with clear dispersion along the  $c$ -axis direction. The intensity of the resonance develops like a superconducting order parameter, and the mode occurs at distinctively different energies at  $(1, 0, 0)$  and  $(1, 0, 1)$ . If the resonance energy is directly associated with the superconducting gap energy  $\Delta$ , then  $\Delta$  is dependent on the wavevector transfers along the  $c$ -axis. These results suggest that one must be careful in interpreting the superconducting gap energies obtained by surface sensitive probes such as scanning tunneling microscopy and angle resolved photoemission.

PACS numbers: 74.25.Ha, 74.70.-b, 78.70.Nx

Understanding the interplay between spin fluctuations and superconductivity in high-transition-temperature (high- $T_c$ ) superconductors is important because spin fluctuations may mediate electron pairing for superconductivity [1, 2]. In the case of high- $T_c$  copper oxides, it is now well documented that the spin fluctuation spectrum is dominated by a collective excitation known as the resonance mode centered at the antiferromagnetic (AF) ordering wavevector  $Q = (1/2, 1/2)$  [3, 4, 5, 6, 7, 8]. Although the intensity of the mode behaves like an order parameter below  $T_c$ , the energy of the mode is dispersionless for wavevector transfers along the  $c$ -axis and directly tracks  $T_c$  [4, 5, 6, 7, 8], thus suggesting that the mode is an intrinsic property of the two-dimensional (2D) CuO<sub>2</sub> planes and intimately associated with superconductivity. For FeAs-based superconductors [9, 10, 11, 12], the presence of static AF ordering in their parent compounds (with spin structure of Fig. 1a) [13, 14, 15, 16, 17, 18] and the remarkable similar doping dependent phase diagram to that of the high- $T_c$  copper oxides [15] suggest that AF spin fluctuations may also play an important role in the superconductivity of these materials. Indeed, recent neutron scattering measurements on spin fluctuations of powder samples of superconducting Ba<sub>0.6</sub>K<sub>0.4</sub>Fe<sub>2</sub>As<sub>2</sub> ( $T_c = 38$  K) [19] and crystalline electric field (CEF) excitations of Ce in CeFeAsO<sub>0.84</sub>F<sub>0.16</sub> ( $T_c = 41$  K) [20] found clear evidence for resonant-like magnetic intensity gain below  $T_c$  at  $\hbar\omega \sim 14$  and 18.7 meV, respectively. However, the Ce CEF measurements give no information on the  $Q$ -dependence of the scattering [20]. Although the resonant-like scattering in Ba<sub>0.6</sub>K<sub>0.4</sub>Fe<sub>2</sub>As<sub>2</sub> occurs near the AF ordering wavevector, the powder nature of the experiment impedes to distinguish whether the resonant scattering is centered at the three-dimensional (3D)

AF wavevector  $Q = (1, 0, 1)$  of its parent compound [16, 17, 18] or simply at a 2D AF in-plane wavevector  $Q = (1, 0, 0)$  [19].

In this Letter, we report the results of inelastic neutron scattering studies of spin fluctuations in single crystals of superconducting BaFe<sub>1.9</sub>Ni<sub>0.1</sub>As<sub>2</sub> (with  $T_c = 20$  K, see Fig. 1c) [12]. We show that the effect of superconductivity is to gradually open a low-energy spin gap and also to induce a resonance at energies above the spin gap energy. Although the intensity of the resonance develops below  $T_c$  similar to that of the resonance in high- $T_c$  copper oxides, the mode actually has a dispersion along the  $c$ -axis, and occurs at distinctively different energies at  $Q = (1, 0, 1)$  and  $(1, 0, 0)$  in contrast with the cuprates. If the resonance energy in FeAs superconductors is associated with  $T_c$  and the superconducting gap energy  $\Delta$ , then  $\Delta$  should be 3D in nature and depend sensitively on the wavevector transfers along the  $c$ -axis. Therefore, one must be careful in interpreting  $\Delta$  obtained by surface sensitive probes such as scanning tunneling microscopy and angle resolved photoemission.

We grew many high quality BaFe<sub>1.9</sub>Ni<sub>0.1</sub>As<sub>2</sub> single crystals (each with mosaicity  $< 0.5^\circ$ ) using flux method as described in Ref. [12]. Figure 1c shows resistivity and magnetic susceptibility data of a typical crystal showing an onset  $T_c$  of 20.2 K with a transition width less than 1 K. We coaligned 21 single crystals on a flat Al plate to obtain a total mass of about 0.6 grams. The in-plane mosaic of the aligned crystal assembly is about  $1.3^\circ$  and the out-of-plane mosaic is less than  $4.3^\circ$  full width at half maximum (FWHM). Our neutron scattering experiments were performed on the PANDA cold triple-axis spectrometer at the Forschungsneutronenquelle Heinz Maier-Leibnitz (FRM II), TU München, Germany. We used

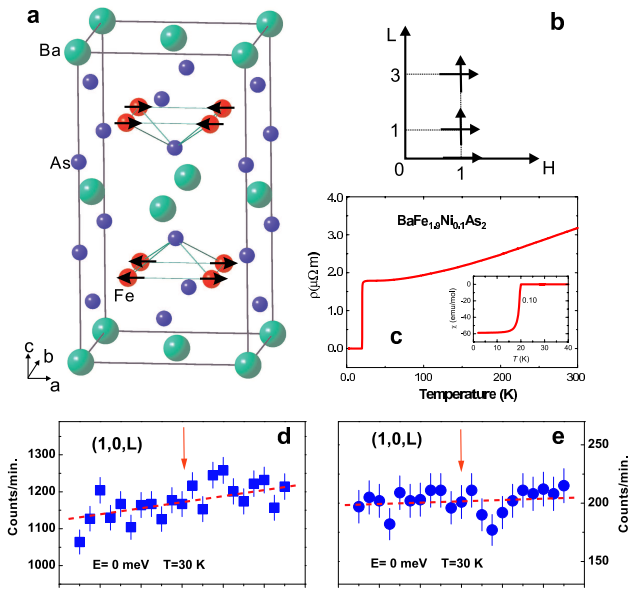


FIG. 1: (color online). (a) Schematic diagram of the Fe spin ordering in the BaFe<sub>2</sub>As<sub>2</sub> and we use the same unit cell for BaFe<sub>1.9</sub>Ni<sub>0.1</sub>As<sub>2</sub> for easy comparison. (b) Reciprocal space probed in our experiment. (c) Resistivity and Magnetic susceptibility measurements of  $T_c$ . (d,e) Elastic neutron scattering  $L$ -scans through (1,0,1) and (1,0,3) magnetic Bragg peaks at 30 K, showing no evidence of static long-range AF order [17, 18].

pyrolytic graphite PG(0,0,2) as monochromator and analyzer without any collimator. For inelastic neutron scattering, monochromator and analyzer were vertically and horizontally focused. For sample alignment and elastic measurements they were both horizontally flat and vertically focused. We defined the wave vector  $Q$  at  $(q_x, q_y, q_z)$  as  $(H, K, L) = (q_x a / 2\pi, q_y b / 2\pi, q_z c / 2\pi)$  reciprocal lattice units (rlu) using the orthorhombic magnetic unit cell previously taken for the magnetic structure determination [16, 17, 18] and the low energy spin wave measurements [21, 22, 23] of the parent undoped compound (space group  $Fmmm$ ,  $a = 5.564$ ,  $b = 5.564$ , and  $c = 12.77$  Å). We choose this reciprocal space notation (although the actual crystal structure is tetragonal) for easy comparison with previous spin-wave and elastic measurements on the parent compound, where magnetic Bragg peaks and low-energy spin waves are expected to occur around (1,0,1) and (1,0,3) rlu positions (see Fig. 1b). For the experiment, the BaFe<sub>1.9</sub>Ni<sub>0.1</sub>As<sub>2</sub> crystal assembly was mounted in the  $[H, 0, L]$  zone inside a closed cycle refrigerator. The final neutron wavevector was fixed at either  $k_f = 1.55$  Å<sup>-1</sup> with a cold Be filter or at  $k_f = 2.662$  Å<sup>-1</sup> with a PG filter in front of the analyzer.

We first searched for possible static AF order in our samples. For undoped BaFe<sub>2</sub>As<sub>2</sub>, magnetic Bragg peaks are expected at the (1,0,1) and (1,0,3) positions for the spin structure of Fig. 1a [16]. In addition, the low tem-

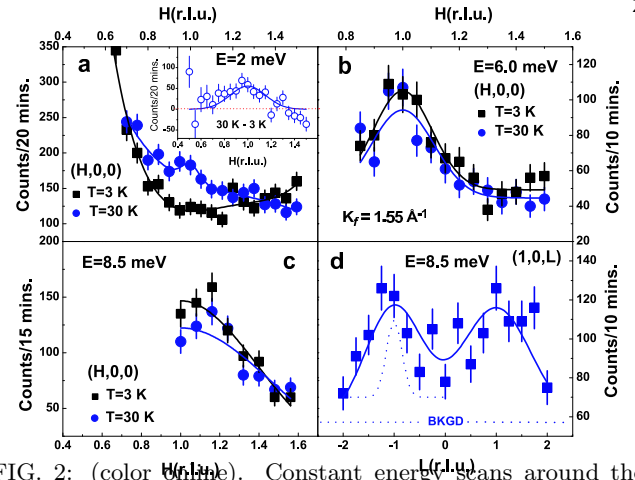


FIG. 2: (color online). Constant energy scans around the (1,0,0) and (1,0,1) positions for  $\hbar\omega = 2, 6,$  and  $8.5$  meV obtained with  $k_f = 1.55$  Å<sup>-1</sup>. (a-c)  $Q$ -scan along the  $[H, 0, 0]$  direction for  $\hbar\omega = 2, 6,$  and  $8$  meV at 30 K and 3 K. The inset in (a) shows the temperature difference plot and a Gaussian fit to the data. The missing low- $Q$  data for scans in (b) and (c) are due to kinematic constraint. (d)  $Q$ -scan along the  $[1, 0, L]$  direction for  $\hbar\omega = 8.5$  meV at 3 K. Note two clear peaks centered at (1,0,-1) and (1,0,1), respectively. The dashed-line peak is the low-temperature spin-waves of BaFe<sub>2</sub>As<sub>2</sub> at  $\hbar\omega = 10$  meV from Fig. 2f in [23].

perature spin waves are gapped below 9.8 meV [23]. Our elastic  $Q$ -scans through these expected AF Bragg peak positions are featureless (Figs. 1d and 1e), confirming the absence of static long-range order above 30 K. Figure 2 summarizes constant-energy scans at 3 K (well below  $T_c$ ) and at 30 K (above  $T_c$ ) at  $\hbar\omega = 2, 6,$  and  $8.5$  meV carried out with  $k_f = 1.55$  Å<sup>-1</sup>. Although these probed energies are well below the 9.8 meV spin gap energy in the parent compound [23], we observe at 30 K clear peaks centered at the in-plane AF wavevector (1,0,0) for  $\hbar\omega = 2$  and 6 meV, and half of a peak at  $\hbar\omega = 8.5$  meV due to kinematic constraints (Figs. 2a-c). Fourier transforms of the gaussian peaks in Figs. 2a and 2b gave the minimum dynamic spin correlation lengths of  $\xi \approx 16 \pm 4$  and  $21 \pm 4$  Å for  $\hbar\omega = 2$  and 6 meV, respectively. The spin-spin correlations extend only to several chemical unit cells and are much smaller than the  $\xi \approx 80 \pm 10$  Å at  $\hbar\omega = 1.5$  meV obtained for electron-doped cuprate superconductor Pr<sub>0.88</sub>LaCe<sub>0.12</sub>CuO<sub>4</sub> [7]. On cooling from the normal ( $T = 30$  K) to the superconducting ( $T = 3$  K) state, the Gaussian peak at  $\hbar\omega = 2$  meV vanishes and suggests the opening of a spin gap (Figs. 2a). In contrast, the Gaussian peaks at  $\hbar\omega = 6$  meV hardly change across  $T_c$  (Fig. 2b) whereas the scattering at (1,0,0) for  $\hbar\omega = 8.5$  meV actually increases below  $T_c$  (Fig. 2c). These results are similar to those for electron-doped Nd<sub>1.85</sub>Ce<sub>0.15</sub>CuO<sub>4</sub> [8], and immediately suggest that the opening of a low-energy spin gap below  $T_c$  is compensated by intensity gain above the gap energy. The low temperature (1,0, $L$ ) scan at  $\hbar\omega = 8.5$  meV shows two broad peaks centered at (1,0,-1) and (1,0,1) corresponding to the 3D AF or-

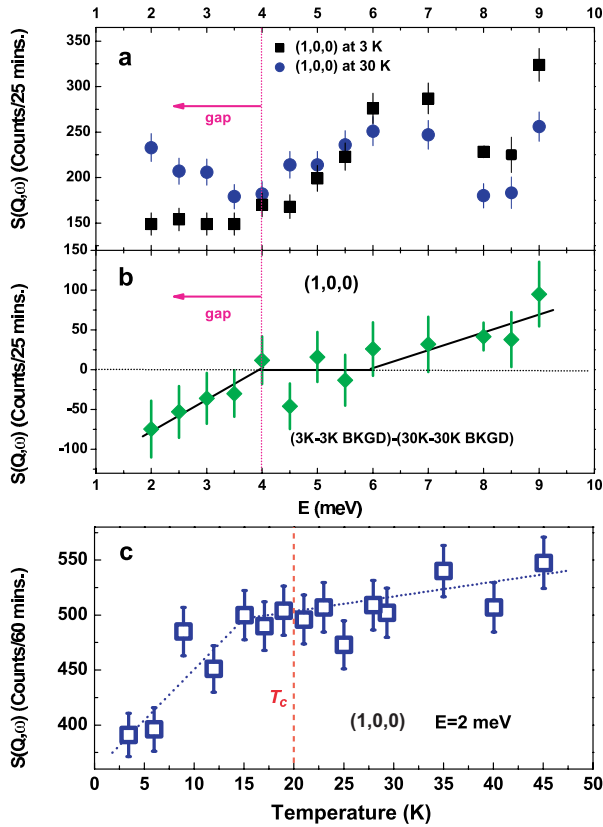


FIG. 3: (color online). Constant- $Q$  scans at the  $(1, 0, 0)$  position above and below  $T_c$  obtained with  $k_f = 1.55 \text{ \AA}^{-1}$  and the temperature dependence of the scattering at  $Q = (1, 0, 0)$  and  $\hbar\omega = 2 \text{ meV}$ . Background scattering was also collected at the  $(1.3, 0, 0)$  position. (a) Energy scans at  $Q = (1, 0, 0)$  from 2 meV to 9 meV at 30 K and 3 K. (b) Background corrected intensity difference between the 3 K and 30 K data at  $Q = (1, 0, 0)$ . The negative scattering below 4 meV indicates the opening of a spin gap, while positive scattering above 6 meV suggests magnetic intensity gain below  $T_c$ . (c) Temperature dependence of the scattering obtained at  $Q = (1, 0, 0)$  and  $\hbar\omega = 2 \text{ meV}$  with vertical dashed line indicating the onset of superconductivity. The  $\hbar\omega = 2 \text{ meV}$  spin gap does not start to open until about 4 K below  $T_c$ .

dering wavevector [16, 17, 18].

To determine the size of the superconducting spin gap and confirm the intensity gain at  $\hbar\omega = 8.5 \text{ meV}$  below  $T_c$ , we carried out energy scans at the in-plane AF wavevector  $Q = (1, 0, 0)$  below and above  $T_c$  (Fig. 3a). While the background scattering collected at  $Q = (1.3, 0, 0)$  (not shown) changes only negligibly between 30 K and 3 K, intensity at  $Q = (1, 0, 0)$  is suppressed for  $\hbar\omega \leq 4 \text{ meV}$  and enhanced for  $\hbar\omega \geq 6 \text{ meV}$  with highest intensity at  $\hbar\omega = 9 \text{ meV}$ . In Fig. 3b we plot the difference (3 K minus 30 K) of the (background corrected) magnetic scattering at  $Q = (1, 0, 0)$ , again confirming the opening of a spin gap for  $\hbar\omega \leq 4 \text{ meV}$  and enhanced magnetic scattering for  $\hbar\omega \geq 6 \text{ meV}$  in the superconducting state. Figure 3c shows the temperature dependence of the scattering at

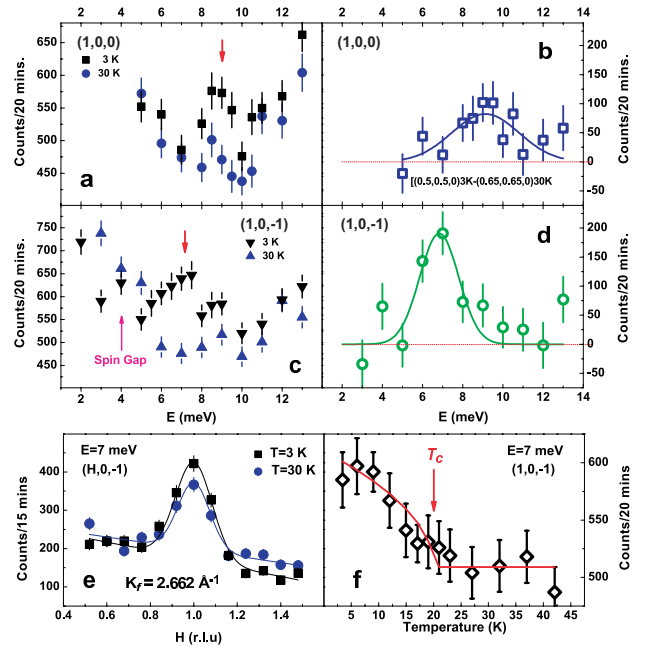


FIG. 4: (color online). Constant energy and constant- $Q$  scans around the  $Q = (1, 0, 0)$  and  $(1, 0, 1)$  positions above and below  $T_c$  obtained with  $k_f = 2.662 \text{ \AA}^{-1}$ . We also collected background scattering at  $Q = (1.3, 0, -1)$  and found it to be temperature independent between 30 K and 3 K for energies above 5 meV (not shown). (a) Energy scans at the 2D AF wavevector  $Q = (1, 0, 0)$  from 5 meV to 13 meV at 30 K and 3 K. Clear magnetic intensity gain is observed at  $\hbar\omega = 9.0 \text{ meV}$ . (b) The temperature difference scattering between 3 K and 30 K shows a clear resonant peak at  $\hbar\omega = 9.1 \pm 0.4 \text{ meV}$ . (c) Energy scans at the 3D AF wavevector  $Q = (1, 0, -1)$  from 2 meV to 13 meV at 30 K and 3 K. The resonance has shifted to  $\hbar\omega = 7 \text{ meV}$  and is about 2.0 meV lower than that at  $Q = (1, 0, 0)$ . (d) The temperature difference plot confirms that the mode has now moved to  $7.0 \pm 0.5 \text{ meV}$ . Note that the intensity gain below  $T_c$  at  $\hbar\omega = 7 \text{ meV}$  and  $Q = (1, 0, -1)$  is just as large as that at  $\hbar\omega = 9.1 \text{ meV}$  and  $Q = (1, 0, 0)$ . (e) Wavevector dependence of the scattering at 30 K and 3 K for  $\hbar\omega = 7 \text{ meV}$ , confirming that the resonance intensity gain occurs at  $Q = (1, 0, -1)$ . (f) Temperature dependence of the scattering obtained at  $Q = (1, 0, -1)$  and  $\hbar\omega = 7 \text{ meV}$  shows clear order parameter like increase below  $T_c$ .

$Q = (1, 0, 0)$  and  $\hbar\omega = 2 \text{ meV}$ . It seems that the suppression of intensity at  $\hbar\omega = 2 \text{ meV}$  does not exactly start at  $T_c$  but about 4 K below  $T_c$ . These results suggest that the spin gap in  $\text{BaFe}_{1.9}\text{Ni}_{0.1}\text{As}_2$  opens gradually with decreasing temperature until it reaches about 4 meV at 3 K, remarkable similar to the spin gap behavior of electron-doped  $\text{Nd}_{1.85}\text{Ce}_{0.15}\text{CuO}_4$  [8, 24].

Although the results displayed in Figs. 1-3 using  $k_f = 1.55 \text{ \AA}^{-1}$  are suggestive of a resonance below  $T_c$ , kinematic constraints did not allow us to carry out measurements for energies above  $\hbar\omega = 9 \text{ meV}$  at  $Q = (1, 0, 0)$ . To determine the energy location of the possible mode, we collected additional data with  $k_f = 2.662 \text{ \AA}^{-1}$ . Figure 4a shows the energy scan raw data at  $Q = (1, 0, 0)$

below and above  $T_c$ . Inspection of the data reveals that the low-temperature scattering enhances dramatically around  $\hbar\omega = 9.0$  meV compared to the normal state scattering. Since Bose population factor does not contribute much to magnetic scattering intensity for  $\hbar\omega \geq 5$  meV between 3 K and 30 K, the (low minus high) temperature difference scattering represents the net magnetic intensity gain at low temperature. Subtracting the 30 K data from the 3 K data reveals a clear localized mode near 9.0 meV (Fig. 4b). Gaussian fit to the data gives a peak position  $\hbar\omega = 9.1 \pm 0.4$  meV, a peak width  $3.3 \pm 0.9$  meV, and an integrated area  $346 \pm 82$  per 20 minutes (Fig. 4b).

Since spin excitations at  $\hbar\omega = 8.5$  meV peak at  $(1, 0, -1)/(1, 0, 1)$  and are clearly dispersive along the  $c$ -axis direction (Fig. 2d), we carried out additional measurements to search for resonance at the 3D AF ordering wavevector  $Q = (1, 0, -1)$  below and above  $T_c$ . The outcome in Fig. 4c shows a large magnetic intensity gain below  $T_c$  at  $\hbar\omega = 7$  meV, clearly different from the 9.1 meV resonance at  $Q = (1, 0, 0)$ . A Gaussian fit to the temperature difference plot in Fig. 4d gives a peak position  $\hbar\omega = 7.0 \pm 0.5$  meV, a peak with  $1.9 \pm 0.7$  meV, and an integrated area of  $464 \pm 145$  per 20 minutes. To further confirm that the intensity gain at  $\hbar\omega = 7$  meV is indeed the resonance occurring at  $Q = (1, 0, -1)$ , we carried constant-energy scans around  $(1, 0, -1)$  and outcome clearly shows that the intensity gain below  $T_c$  arises from scattering at the 3D AF ordering position (Fig. 4e). Finally, in Fig. 4f we plot the temperature dependence of the scattering at  $(1, 0, -1)$  and  $\hbar\omega = 7$  meV. The scattering increases dramatically below the onset of  $T_c$  and is remarkably similar to that of the resonance in high- $T_c$  copper oxides [3, 4, 5, 6, 7, 8].

If the resonance is a measure of electron pairing correlations in high- $T_c$  superconductors [25], the observed 3D resonance dispersion in  $\text{BaFe}_{1.9}\text{Ni}_{0.1}\text{As}_2$  would suggest a variation of the superconducting energy gap  $\Delta$  along the  $c$ -axis. This is quite different from the high- $T_c$  copper oxides, where  $\Delta$  is strictly 2D and independent of the  $c$ -axis modulations. For FeAs-based superconductors, the resonance may arise from quasiparticle transitions across the sign-revised  $s$ -wave electron ( $\Delta_e^0$ ) and hole ( $\Delta_h^0$ ) superconducting gaps in pure two dimensional models [26, 27, 28, 29, 30, 31]. By considering the AF coupling between layers, the gap functions can be naturally modified to  $\Delta_e(k_z) = \Delta_e^0 + \delta \cos(k_z)$  and  $\Delta_h(k_z) = \Delta_h^0 + \delta \cos(k_z)$ . For a sign-revised  $s$  pairing symmetry,  $\Delta_e^0 \sim -\Delta_h^0 \sim -\Delta_0$ . Therefore, the dispersion of the resonance along  $c$ -axis is roughly determined by [27]

$$\begin{aligned} \hbar\omega(q_z) &\sim \text{Min}(\langle |\Delta_e(k_z)| + |\Delta_h(k_z + q_z)| \rangle, k_z) \\ &\sim 2\Delta_0 - 2\delta \left| \sin\left(\frac{q_z}{2}\right) \right| \end{aligned} \quad (1)$$

Based on this interpretation, our experimental results

suggest  $\delta/\Delta_0 = [\omega(1, 0, 0) - \omega(1, 0, -1)]/\omega(1, 0, 0) = 0.26 \pm 0.07$ . If spin fluctuations are responsible for electron pairing and superconductivity, the values  $\Delta_0$  and  $\delta$  are expected to be proportional to the intra-plane and inter-plane AF couplings,  $J_{\parallel}$  and  $J_{\perp}$ , respectively, which naturally suggests  $\delta/\Delta_0 \sim J_{\perp}/J_{\parallel}$ . The ratio  $\delta/\Delta_0$  determined by our resonance dispersion is reasonable agreement with the ratio of the AF exchange couplings measured by neutron scattering experiments in the parent compounds[21, 22, 23]. These results suggest that spin fluctuations are also important for superconductivity in FeAs-based superconductors.

This work is supported by the U.S. NSF No. DMR-0756568, U.S. DOE BES No. DE-FG02-05ER46202, and in part by the U.S. DOE, Division of Scientific User Facilities. The work at Zhejiang University is supported by the NSF of China. We further acknowledge support from DFG within Sonderforschungsbereich 463 and from the PANDA project of TU Dresden and FRM II.

Note added: After independently finishing the experimental part of the present paper, we became aware of a similar neutron scattering experiment, where the resonance at  $\hbar\omega = 9.5$  meV was discovered near  $Q = (1, 0, 0)$  [ $(1/2, 1/2, 0)$  in tetragonal notation] in single crystal superconducting  $\text{BaFe}_{1.84}\text{Co}_{0.16}\text{As}_2$  ( $T_c = 22$  K) [32].

---

\* Electronic address: daip@ornl.gov

- [1] D. J. Scalapino, Phys. Rep. **250** 330 (1995).
- [2] A. Abanov *et al.*, J. Electron Spectrosc. Relat. Phenom. **117-118**, 129 (2001).
- [3] J. Rossat-Mignod *et al.*, Physica C **185**, 86 (1991).
- [4] H. A. Mook *et al.*, Phys. Rev. Lett. **70**, 3490 (1993).
- [5] C. Stock *et al.*, Phys. Rev. B **69**, 014502 (2005).
- [6] H. F. Fong *et al.*, Nature (London) **398**, 588 (1999).
- [7] S. D. Wilson *et al.*, Nature (London) **42**, 59 (2006).
- [8] J. Zhao *et al.*, Phys. Rev. Lett. **99**, 017001 (2007).
- [9] Y. Kamihara *et al.*, J. Am. Chem. Soc. **130**, 3296 (2008).
- [10] M. Rotter *et al.*, Phys. Rev. Lett. **101**, 107006 (2008).
- [11] A. S. Sefat *et al.*, Phys. Rev. Lett. **101**, 117004 (2008).
- [12] L. J. Li *et al.*, arXiv: 0809.2009v1.
- [13] C. de la Cruz *et al.*, Nature (London) **453**, 899 (2008).
- [14] M. A. McGuire *et al.*, Phys. Rev. B **78**, 094517 (2008).
- [15] J. Zhao *et al.*, Nature Materials **7**, 953 (2008).
- [16] Q. Huang *et al.*, arXiv:0806.2776.
- [17] J. Zhao *et al.*, Phys. Rev. B **78**, 140504(R) (2008).
- [18] A. I. Goldman *et al.*, Phys. Rev. B **78**, 100506(R) (2008).
- [19] A. D. Christianson *et al.*, Nature (London) (in press).
- [20] Songxue Chi *et al.*, Phys. Rev. Lett. **101**, 217002 (2008).
- [21] J. Zhao *et al.*, Phys. Rev. Lett. **101**, 167203 (2008).
- [22] R. J. McQueeney *et al.*, Phys. Rev. Lett. **101**, 227205 (2008).
- [23] K. Matan *et al.*, arXiv: 0810.4790v1.
- [24] K. Yamada *et al.*, Phys. Rev. Lett. **90**, 137004 (2003).
- [25] Pengcheng Dai *et al.*, Nature (London) **406**, 965 (2000).
- [26] I. I. Mazin *et al.*, Phys. Rev. Lett. **101**, 057003 (2008).
- [27] T. A. Maier and D. J. Scalapino, Phys. Rev. B **78**, 020514(R) (2008).

- [28] M. M. Korshunov and I. Eremin, Phys. Rev. B **78**, 140509(R) (2008).
- [29] A. V. Chubukov, D. V. Efremov, and I. Eremin, Phys. Rev. B **78**, 134512 (2008).
- [30] K. Seo *et al.*, Phys. Rev. Lett. **101**, 206404 (2008).
- [31] F. Wang *et al.*, arXiv:0807.0498.
- [32] M. D. Lumsden *et al.*, arXiv: 0811.4755v1.